

Rain Attenuation and Doppler Shift Compensation for Satellite Communications

Sooyoung Kim Shin, Kwangjae Lim, Kwonhue Choi, and Kunseok Kang

In high-speed multimedia satellite communication systems, it is essential to provide high-quality, economical services by using efficient transmission schemes which can overcome channel impairments appearing in the satellite link. This paper introduces techniques to compensate for rain attenuation and the Doppler shift in the satellite communication link. An adaptive transmission technique with a control algorithm to adaptively allocate transmission schemes is used as a countermeasure to rain attenuation. We introduce a new rain attenuation modeling technique for estimating system performance and propose a novel Doppler shift compensation algorithm with reduced hardware complexity. Extensive simulation results show that the proposed algorithm can provide greatly enhanced performance compared to conventional algorithms. Simulation software and hardware which incorporate the proposed techniques are also demonstrated.

I. INTRODUCTION

The demand for high-speed wireless multimedia service is rapidly growing worldwide because of tremendous economic development and the resultant enhanced living standards. The introduction of high-speed satellite communication systems is a response to the high demand for wireless multimedia services of various forms. One solution to the limitations of terrestrial wireless communications, such as geographical limitations, would be a satellite communication system using either geostationary or non-geostationary orbits. Satellite communication service would be highly efficient and economical because of advantages such as a wide area of coverage and a flexibility of network configuration; these cannot be provided by terrestrial communication networks.

One of the main problems in providing high-speed services in satellite communication systems is rain attenuation. This is because a high frequency band is mandatory for providing high-speed wideband multimedia services, and rain attenuation is one of the most critical factors in degrading satellite link quality. In addition, when a service uses non-geostationary orbit satellites, the Doppler shift is also a critical factor in reducing spectral efficiency. In fact, many wideband, high-speed satellite communication systems under development use non-geostationary orbits: for example, SkyBridge [1] and Teledesic [2]. A large power margin must be used to overcome these problems. However, this requires expensive hardware at the satellite earth stations and high power consumption at user terminals, thus further increasing service charges. This situation calls for efficient transmission schemes which can provide economical communication services; one of the strongest candidates is an adaptive transmission scheme with Doppler shift compensation ability. Such a scheme should have a simple

Manuscript received June 18, 2001; revised Oct. 24, 2001.

This work was supported in part by the Korean Ministry of Information and Communication. Sooyoung Kim Shin (phone: +82 42 860 4907, e-mail: sookim@etri.re.kr), Kwangjae Lim (e-mail: kjlim@etri.re.kr), Kwonhue Choi (e-mail: khchoi@etri.re.kr), and Kunseok Kang (e-mail: kangks@etri.re.kr) are with Satellite Transmission Technology Team, ETRI, Daejeon, Korea.

structure and the ability to effectively compensate for rain attenuation and the Doppler shift.

The non-geostationary satellite channel for high speed communications cannot be considered an additive white Gaussian noise (AWGN) channel because of signal fading due to rain and the Doppler shift on the channel. For these reasons, we developed our own rain attenuation model with which we can synthesize the dynamic characteristics of rain attenuation. Carrier offset induced by the Doppler shift is also modeled by the orbit constellation parameters of a non-geostationary orbit satellite system.

A simple and efficient estimation and prediction algorithm for channel conditions was required for allocating suitable transmission schemes at each sampling time. We developed various control algorithms and estimated their performance using the rain attenuation model.

This paper proposes an efficient transmission system which can be adaptively applied in rain attenuation situations. Our system uses a block turbo code with an M-ary phase shift keying (PSK) strategy and for Doppler shift compensation, a 2-dimensional search algorithm which uses fast Fourier transform (FFT). Because of the successful development of code division multiple access (CDMA) technology for terrestrial mobile communications [3], application of CDMA to satellite communication is now being attempted. We developed a CDMA-based Doppler shift compensation technique to conform to this technological trend.

In section II, we briefly present a simulation modeling technique for rain attenuation and the Doppler shift on the satellite communication channel. Section III describes the adaptive transmission scheme and the Doppler shift compensation method, and demonstrates simulation results using our own developed simulation software (S/W) packages. Section IV introduces a hardware (H/W) emulation board with an adaptive rain attenuation compensation algorithm. Finally, conclusions are drawn in section V.

II. CHANNEL MODEL

1. Rain Attenuation Model

We previously developed a rain attenuation model with which we can synthesize time-varying rain attenuation for any given time interval at Ku and Ka frequency bands [4]. This was necessary so that we could estimate the performance of the proposed adaptive compensation algorithm.

Several papers have presented techniques on dynamic rain attenuation modeling [5]-[7]. Because Korea experiences heavy rain during a short period, it was difficult to synthesize rain attenuation. Therefore, we believed it necessary to develop a rain attenuation model which could synthesize typical Korean

rain attenuation dynamics. The rain attenuation model we developed used measured attenuation data from the 12.25 GHz beacon signal of Koreasat 2 for two years; an example is shown in Fig. 1. Motivated by the fact that rain attenuation is a Markov process, a Markov chain [8] was used to model the rain attenuation process. We assumed that a rain event could be characterized by a 4-state Markov-chain. That is, a rain event consists of a beginning, a fading, an ending and an inter-fade state with a duration of b_D, f_D, i_D and e_D , respectively, as shown in Fig. 1, and Fig. 2 shows a corresponding 4-state Markov chain. In Fig. 2, p_x is the transition probability of a state changing from state x , and A is attenuation.

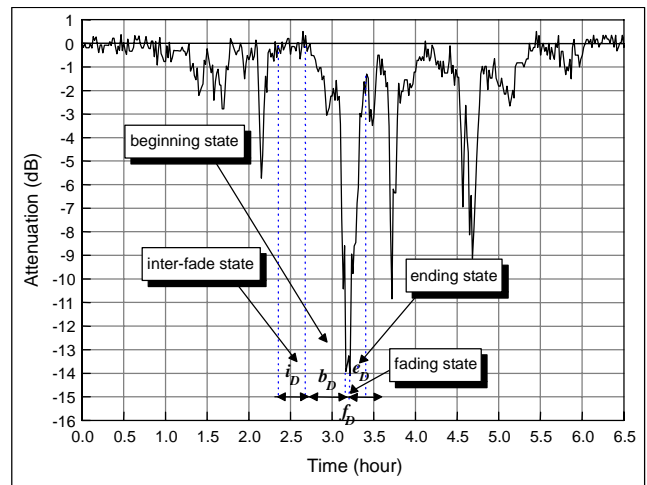


Fig. 1. An example of measured rain attenuation data characterized by 4 states.

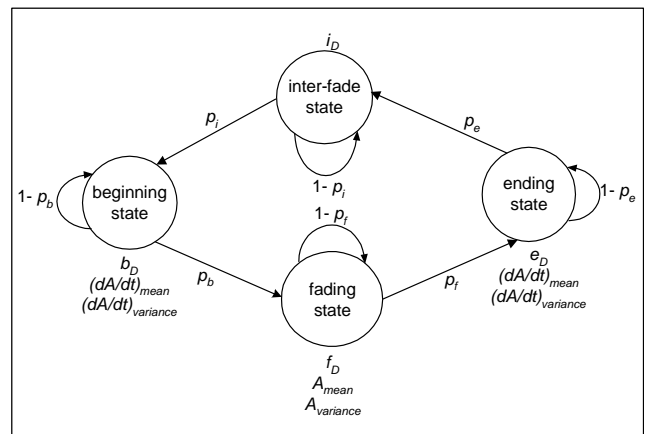


Fig. 2. 4-state Markov chain for rain attenuation process.

Our rain attenuation synthesizing process applies not only the state parameters but also the relationships between them. A more detailed procedure for modeling the rain attenuation process can be found in [4]. Figure 3 shows an example of synthesized rain attenuation data using the proposed model, and

Fig. 4 shows a comparison of the statistics of synthesized and measured rain attenuation data. As Figs. 3 and 4 show, the probability distributions of the synthesized data approximate those of the measured ones.

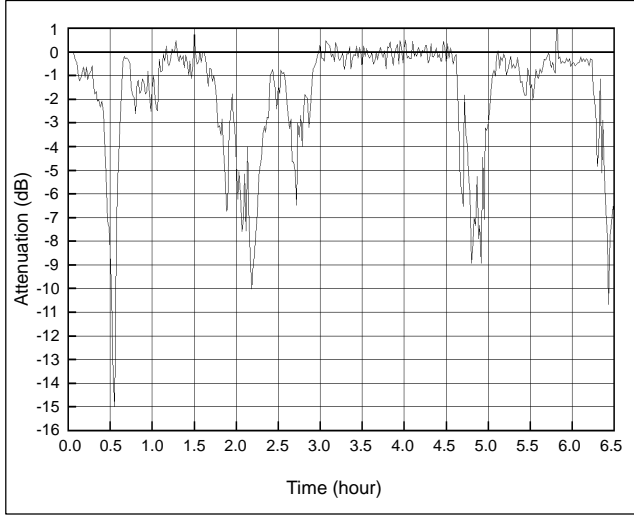


Fig. 3. An example of synthesized rain attenuation data.

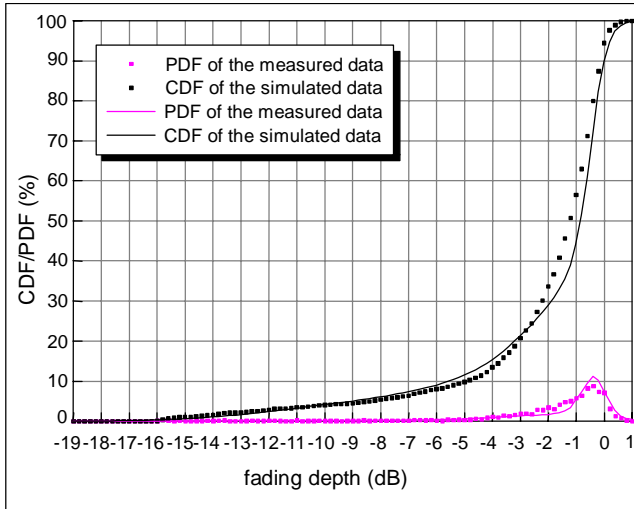


Fig. 4. Probability density function (PDF) and cumulative probability density function (CDF) of synthesized and measured rain data.

We applied a time interpolation technique using the Random Midpoint Displacement algorithm [9] to generate rain attenuation data for any time interval and a frequency scaling method recommended by ITU-R. Detailed results of time interpolation of rain attenuation data can be found in [10].

2. Modeling the Doppler Shift

One of the key features of low earth orbit (LEO) satellite systems is the fast changing geometry between the satellite and the

users on the ground. This means that user terminals experience a significant and time-varying Doppler shift, which must be estimated and compensated for to obtain reliable communication. The Doppler shift frequency changes as the satellite passes over, and its value depends on the position of the terminal. In a circular orbit, the Doppler shift is given by [11]

$$F_D = \frac{f_0}{c} \left[\sqrt{\frac{\mu r_E^2}{(r_E+h)^3}} \cos \gamma \sin \varphi - \frac{2\pi}{T_R} r_E \cos l_t \cos \gamma \cos \varphi \right] \quad (1)$$

where f_0 is the carrier frequency, c the speed of light, μ the gravitational constant, r_E the radius of the earth, h the altitude of the satellite orbit, γ the elevation look angle, φ the angle between the projection of the satellite-terminal line onto the tangential plane at the subsatellite point, T_R the earth's rotation period, and l_t the latitude of the terminal location. Figure 5 shows the Doppler shift characteristics of the Iridium satellite system [12] with an altitude of 780 km and orbital slope of 86.4 degrees, for several satellite longitudes θ . The design of the acquisition range and loop dynamics of the Doppler shift recovery must consider the maximum value and the change rate of the Doppler shift for all possible cases of the satellite trajectory. From (1), we can see that the Doppler frequency is proportional to the carrier frequency f_0 . Therefore, a larger acquisition range and higher tracking speed is necessary in order to compensate for the Doppler shift in high frequency band systems operating Ka or Ku bands.

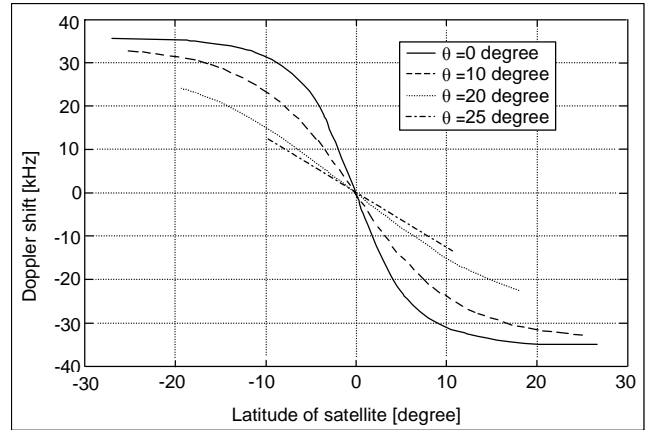


Fig. 5. Doppler shift characteristics of Iridium satellite system for satellite longitudes θ .

III. COMPENSATION TECHNIQUES AND S/W SIMULATION RESULTS

1. Adaptive Transmission Schemes and Algorithms for Rain Attenuation Compensation

Many studies have investigated adaptive transmission schemes

to compensate for rain attenuation, including adaptive coding and modulation schemes [7],[13],[14] and control algorithms [15]. Recently, ETRI also proposed many new adaptive transmission algorithms to compensate for rain attenuation. These include an adaptive coding scheme using block turbo codes [16] and an adaptive CDMA using a parallel combinatory processor [17]. We have also developed intelligent control algorithms to adaptively allocate transmission schemes by estimating and predicting rain attenuation [18].

The system employs spectrally efficient transmission schemes in clear sky conditions and switches them to power-efficient schemes in rainy conditions. In other words, the system allocates additional resources (frequency, time, code, etc.) to a faded user. Since the switching operation involves investigating the history of the received signal quality and predicting the signal quality of the next sampling point, an intelligent control method is required.

The control mechanism consists of signal to noise ratio (SNR) estimation, SNR prediction, and radio format selection [18]. SNR prediction, on the receiving side, must consider the round trip delay on a satellite link. The radio format selection is for adaptively allocating suitable transmission schemes, such as coding and modulation schemes, to both the transmission and receiving sides [19].

A. Proposed Control Algorithms

In order to allocate transmission schemes adaptively according to the channel conditions, it is essential to estimate channel quality. We modified the “method of the mean” [20] to estimate the SNR of received symbols in the M-ary PSK system [18]¹⁾. The histogram of the received symbol is investigated and the proposed estimation scheme then estimates the SNR from the linear combination of the histogram with quadratic weighting factors, which has been verified to perform better than the conventional scheme using linear weighting factors.

In this paper, we assume that 9600 symbols are transmitted in a frame and the switching of the modulation scheme is made on a frame basis. The histogram of the received symbol distribution can be made by counting the number of symbols in each quantization level. By giving proper weighting factors to the histogram, we can get a desirable estimate characteristic, which is monotonically decreasing with an increasing SNR, that is,

$$L_w = f(\text{SNR}), \quad (2)$$

where L_w is the linear combination of the histogram with

¹⁾ This is the international collaborative research result between ETRI and Centre for Communication Systems Research, University of Surrey, U.K.

quadratic weighting factors. Since it is difficult and complex to solve the inverse function f^{-1} to get an SNR value from the L_w , we implemented the inverse transformation by using a look-up table.

The adaptive rain fade compensation system is required to predict in advance with consideration of the round-trip delay the amount of rain attenuation or the signal quality. The SNR variation in a satellite link includes variation of rain attenuation and comparatively fast scintillation. Because, generally, the SNR variation due to scintillation is much faster than the response speed of an adaptive system, the prediction scheme needs to filter out this fast variation. We developed an efficient prediction scheme [18] that consists of four functions including discrete-time low-pass filtering (LPF), rain-fade prediction, mean-error correction and hybrid fixed/variable prediction margin allocation.

In the proposed prediction scheme, an LPF is used to remove the fast variation of the SNR. The scheme then predicts the signal level, y_{t+p} , after a prediction time, p , from the previous signal levels, using the following generic linear regressive filtering:

$$\tilde{y}_{t+p} = \sum_{i=0}^{n-1} w_{i,t} y_{t-i}, \quad (3)$$

where n is an observation time and y_t is the LPF output.

One of the simplest implementations of (3) uses two constant weight values for two end points of the observation period, $w_{0,t} = p/(n-1) + 1$ and $w_{n-1,t} = -p/(n-1)$ and assumes that future variation of the signal level will remain the same as the previous variation. We refer to this method as *slope based prediction* (SBP). On the other hand, variable weights can be employed using adaptive filtering prediction (AFP) algorithms such as the least mean square (LMS) or recursive least square (RLS) [21]. In this case, the weights are updated at each sampling time.

The mean-error correction with a marginal value is used to compensate for prediction error. The marginal value is necessary because of the filtering process for the fast variation of the signal level in the prediction scheme, and it is the sum of a fixed margin and a variable margin obtained from the standard deviation of prediction errors.

For adaptive rain compensation, a real time algorithm is required for selecting an appropriate transmission scheme with the best spectral efficiency and performance under the current attenuation level. At the same time, it should be considered that the switching causes bandwidth overhead due to control information exchange. The proposed selection algorithm [19] selects a transmission scheme, d , having the maximum throughput under a current SNR such that

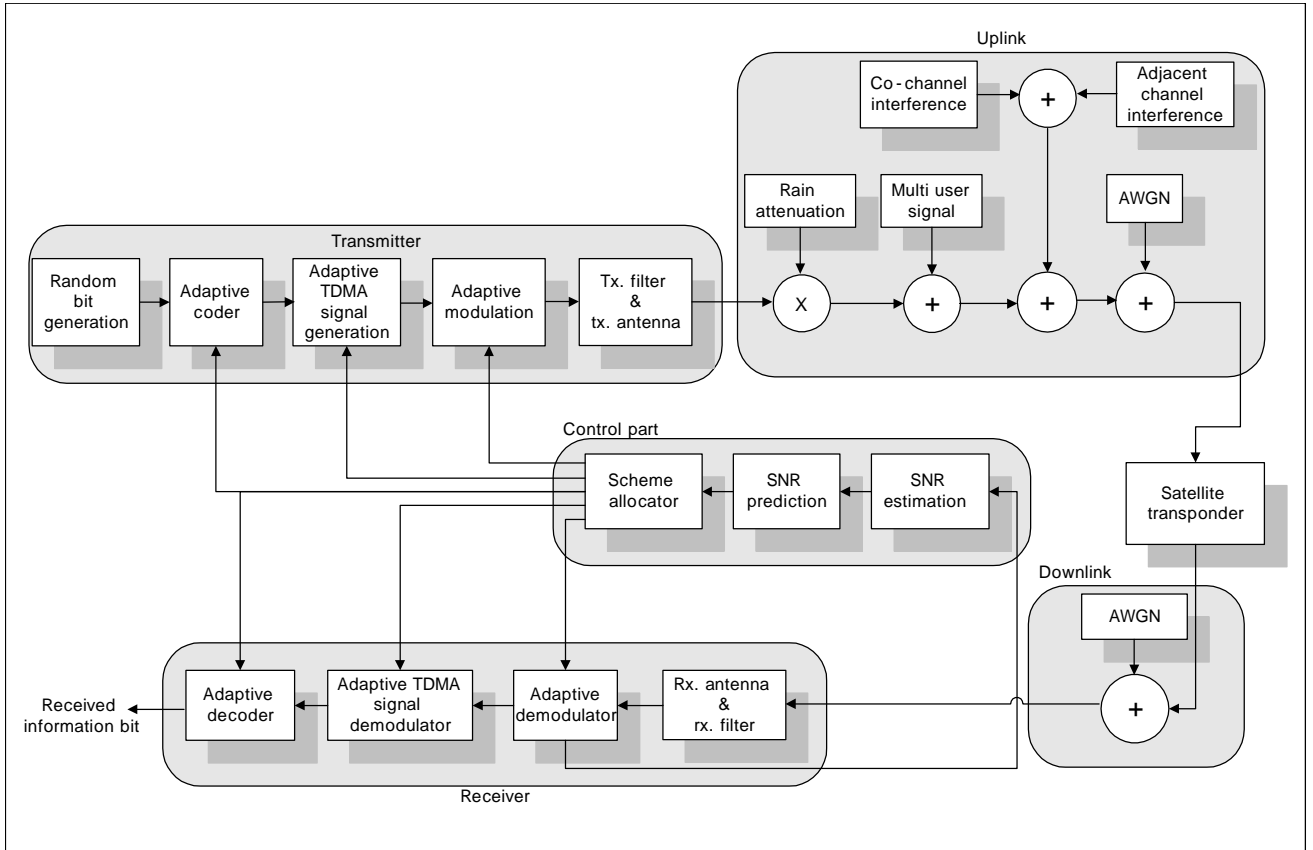


Fig. 6. An example of simulation system using the proposed adaptive rain attenuation compensation algorithms.

$$\arg \max_d \left[\sum_{k=0}^{N-1} \lambda^k S_d(t-k) \right] \text{ for } d \in \{0, 1, \dots, d_{\max} - 1\}, \quad (4)$$

where d_{\max} is the number of available transmission schemes and $S_d(t)$ is the throughput normalized by the data rate of the transmission scheme d . The throughput is obtained by $S_d(t) = 1 - P_d(\gamma(t))$, where $P_d(\gamma(t))$ is the bit error rate (BER) value for the predicted SNR, $\gamma(t)$. When $P_d(\gamma(t))$ is larger than the required BER, the BER is replaced by the value of 1 in order to give a penalty to the selected scheme. To take a time hysteresis into consideration, the throughput value is accumulated for the previous period of length N with weighting factor λ . This weighting factor is determined to be inversely proportional to the current SNR slope as follows:

$$\lambda = \frac{1}{x |\Delta\gamma(t)| + 1}, \quad (5)$$

where $\Delta\gamma(t)$ is the current SNR slope and x is a parameter that adjusts the sensitivity of λ to the slope.

As the SNR level increases, the algorithm may immediately switch to a scheme with a higher data rate to maintain the

highest throughput satisfying the required BER. However, in this case, service outage can be caused if the SNR quickly decreases below a certain level. The algorithm uses a holding timer to prevent this. It admits switching to the transmission scheme with a higher priority only if the scheme is continuously selected during a predefined period.

B. Simulation System Configuration

Figure 6 shows the simulation system we designed to estimate the performance of the proposed rain attenuation compensation technique. We used our rain attenuation model to simulate the performance of the proposed algorithm. In the simulation, the adaptive modulator and demodulator select one of M-ary PSK schemes according to the control signal that is produced by the selection algorithm. Five M-ary PSK schemes of 8-ary PSK, QPSK, BPSK, 2SR (symbol repetition)-BPSK, and 4SR-BPSK were used in the simulation. The former scheme has higher priority than the latter one because of its higher channel efficiency but requires a higher SNR level to satisfy the required BER. For example, the minimum SNR values that satisfy the required BER of 10^{-4} are 2.4 dB, 5.4 dB, 8.4 dB, 11.5 dB and 16.5 dB.

Table 1. System parameters.

| Simulation system parameters | |
|--|------------------------------|
| Simulation time | 345,600 seconds (96 hours) |
| Symbol rate | 9,600 symbols/second |
| Link margin | 3 dB |
| Frequency | 12.5 GHz |
| Required BER | 10^{-4} |
| Rain attenuation | |
| Maximum fading depth | -16.25 dB |
| Fading rate (mean fade slope) | 0.24 dB/second |
| SNR estimation | |
| Observation length | 9,600 symbols |
| Number of quantization levels | 16 |
| SNR prediction | |
| Prediction time | 3 seconds |
| Prediction method | SBP and AFP |
| Observation time (n in (3)) | 3 (for SBP) and 10 (for AFP) |
| Fixed prediction margin | 0.5 dB |
| Adaptive transmission scheme selection | |
| Accumulation length | 5 seconds |
| Max holding time | 5 seconds |

Our simulation focused on the performance of the control algorithms, and thus we did not include adaptive coding scheme because of simulation speed. Table 1 shows system parameters used for the simulation. In the simulation, a time series of rain attenuation data was generated using the model in Section II.1. The important parameters which represent the dynamic characteristics of rain attenuation, such as maximum fading depth and mean fade slope, denoted as Fading rate, are listed in Table 1.

The parameters have also been optimized through extensive simulations. For the SNR estimation, an observation length of 9600 symbols was used; this corresponds to a time duration of one second so that the estimation is performed per second. For the SNR prediction, two types of prediction methods, SBP and AFP, were used. In the AFP, ten weighted values were updated using a normalized LMS (NLMS) algorithm [21].

C. Simulation Results

We first obtained the performance of the proposed SNR estimation algorithm. Figure 7 shows the mean and standard

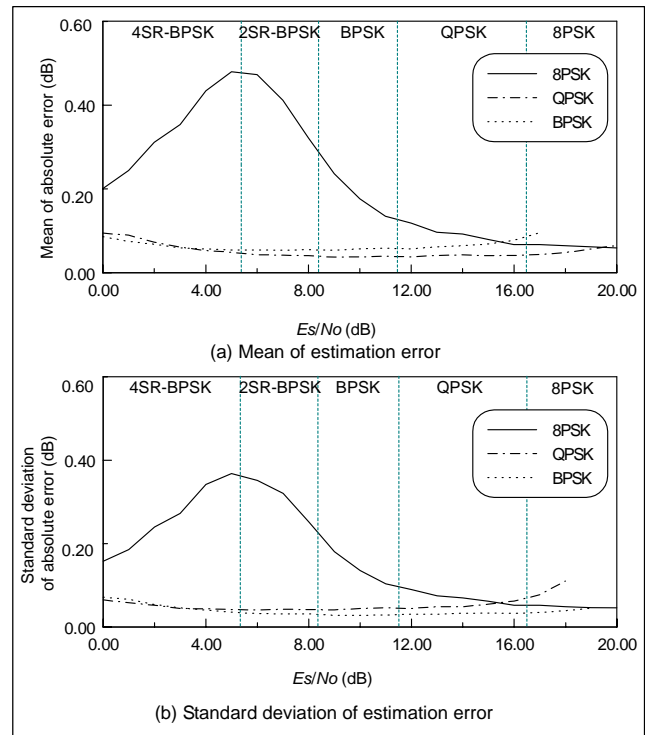


Fig. 7. Performance of the proposed SNR estimation algorithm.

deviation of the absolute values of the estimation error, which is the difference between the real SNR and the estimated SNR, which are denoted by E_s/N_o . The vertical dotted lines in Fig. 7 represent the minimum SNR values that satisfy the required BER of 10^{-4} for five modulation schemes. For each region divided by the lines, a modulation scheme is selected by the selection algorithm. For example, in the rightmost region, 8-ary PSK may be selected and its estimation error for this region should be as small as possible. The simulation results shown in Fig. 7 reveal that the mean and standard deviation of the estimation error are less than 0.1 dB in the operating range of each M-ary PSK. The extensive simulation results for all the PSK schemes used in this study also showed that the estimation error was always less than 0.1 dB in the wide range of SNR for the required BER of 10^{-3} to 10^{-6} .

Table 2 shows the mean and standard deviation of the absolute values of the prediction error, which is the difference between the estimated SNR and the predicted SNR. Table 2 shows that the AFP algorithm experiences the smallest prediction error, although the difference between this prediction error and other prediction algorithms is small. The prediction error was comparatively large when only LPF was used. Simulation results showed that the prediction scheme for the slow variation of rain attenuation does not need to be such a complex algorithm as the AFP.

Table 3 shows the performance of the proposed selection al-

Table 2. Performance of the proposed SNR prediction algorithm in terms of prediction error.

| Algorithm | SBP | AFP by NLMS | Only LPF |
|--------------------|-------|-------------|----------|
| Prediction error | | | |
| Mean | 0.511 | 0.507 | 0.519 |
| Standard deviation | 0.328 | 0.321 | 0.360 |

Table 3. Performance of selection algorithms.

| Algorithm | Proposed | Multi-threshold |
|-------------|-----------------------|-----------------------|
| Performance | | |
| BER | 1.95×10^{-6} | 2.08×10^{-6} |
| Throughput | 25.8 kbps | 25.9 kbps |
| Outage rate | 5.79×10^{-5} | 6.37×10^{-5} |
| Change rate | 2.4×10^{-3} | 4.1×10^{-3} |

Table 4. The performance of adaptive rain attenuation compensation system compared with fixed transmission schemes.

| Scheme | Adaptive | BPSK(fixed) | QPSK(fixed) | 8-PSK(fixed) |
|-------------|-----------------------|-----------------------|-----------------------|-----------------------|
| Performance | | | | |
| BER | 1.95×10^{-6} | 2.47×10^{-5} | 2.31×10^{-4} | 1.79×10^{-3} |
| Throughput | 25.8 kbps | 9.6 kbps | 19.2 kbps | 28.7 kbps |
| Outage rate | 5.79×10^{-5} | 11.1×10^{-5} | 29.6×10^{-5} | 0.219 |

gorithm compared with a simple multi-threshold algorithm which uses required minimum SNR values as the threshold for switching to each transmission method without any hysteresis mechanism. The throughput represents the number of successfully received bits per second. The system is considered to be in outage when the instantaneous BER exceeds the required BER of 10^{-4} . The change rate represents an average number of switching per second, and it is only meaningful for the adaptive compensation scheme. The proposed algorithm has comparable performance to the multi-threshold algorithm in terms of BER, throughput, and outage rate. For the change rate, the proposed algorithm shows an enhanced performance of about two times compared to the multi-threshold one; thus the system overhead can be reduced.

Table 4 shows the performance of the proposed adaptive rain attenuation compensation scheme consisting of SNR estimation, prediction with SBP, and selection algorithms. For comparison, the performance of fixed transmission schemes is also

shown in Table 4. We can easily see that the performance of the adaptive system is superior to that of the fixed transmission system; this is due to the intelligent switching mechanism, which switches according to the SNR variation. For example, the adaptive scheme can improve BER performance one, two, and three orders of magnitude over the BPSK, QPSK, and 8-ary PSK schemes, respectively. Outage performance also can be enhanced at least by 50% with the adaptive scheme. Although the fixed 8-ary PSK scheme shows about a 10% larger throughput than the adaptive system, its performance is significantly inferior in BER and outage to the adaptive scheme. Reference [22] reported similar results. However, the adaptive scheme needs the exchange of a signaling message between a transmitter and a receiver and thus results in overhead in the satellite link.

2. Doppler Shift Compensation

Much of the literature has been devoted to Doppler shift acquisition algorithms for LEO satellite communication systems. Especially for DS-CDMA satellite communication systems, two-dimensional (2-D) search algorithms [23]-[25] have been considered where the acquisition for the Doppler shift and PN code phase is jointly accomplished. Reference [26] proposed a simple and efficient compensation algorithm for residual frequency error after coarse acquisition via 2-D search process. A simple additional computation exploiting the existing structure used for the 2-D search algorithm obtains an estimate of the residual frequency error for fine tracking. We developed a simulator for a Doppler shift compensation system using an enhanced version of the 2-D search algorithm along with the fine tracking algorithm presented in [26]. In this section, we first briefly describe our proposed Doppler shift compensation algorithm. Then, we present the simulation results obtained from our proposed simulator for the Doppler shift compensation system.

A. Developed Doppler Shift Compensation Algorithm

The proposed algorithm first computes the spectral power distribution of pilot channel signal sampled by its chip rate. Then the carrier frequency offset is estimated from the power difference of the two FFT output components adjacent to the component corresponding to the zero frequency offset. For the delay-locked loop, the timing phases of the “early” and “late” local reference PN codes are typically separated from those of the “on-time” code by half of the chip duration. The zero-padding method [24] obtains a similar design for the carrier frequency offset estimation.

Figure 8 shows the Doppler compensation loop structure employing the proposed carrier frequency offset estimation algorithm for Doppler compensation after the 2-D search. After

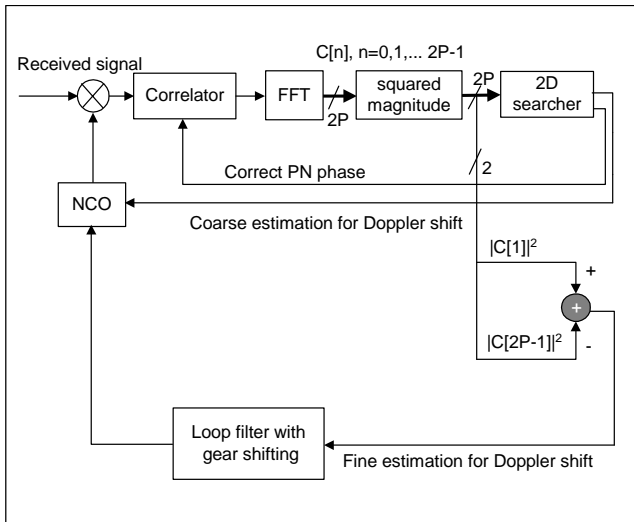


Fig. 8. Structure of the Doppler shift compensation loop employing the developed carrier frequency offset estimation algorithm for fine compensation.

the PN code timing acquisition and coarse Doppler shift compensation, the complex signal is sampled by its chip rate and is fed to the PN correlator and the P correlator output is fed to the $2P$ -point FFT. The FFT output is computed as follows:

$$C[k] = \sum_{n=0}^{P-1} c[n] e^{-j\pi kn/P}, \quad k = 0, 1, 2, \dots, 2P-1 \quad (6)$$

where $c[n]$ is the n -th correlator output. Therefore, the power of $C[k]$ has a characteristic close to the autocorrelation characteristic of a PN code. Based on the similarity, the carrier frequency offset can be estimated as follows:

$$\Delta\hat{f} = |C[1]|^2 - |C[2P-1]|^2. \quad (7)$$

In high frequency band mobile satellite systems, the initial carrier frequency offset that is left by coarse acquisition may have a wide range in the uncertain region because the initial Doppler shift is generally large and unknown. This is because a user will experience various ranges of Doppler shift due to dynamic satellite trajectories. As an efficient solution for the wide range of initial frequency error after coarse acquisition, the proposed algorithm uses the gear-shifting technique, where the loop filter bandwidth at the initial tracking stage is designed to be larger than the remaining tracking stage in order to speed-up the initial frequency tracking.

B. Hardware Complexity of the Proposed Algorithm

To assess the performance of the frequency detector (FD), we introduce FD output SNR as a performance measure,

which is defined as follows:

$$\text{FD output SNR} = \frac{E \left[\left(\frac{d\Delta\hat{f}}{df} \Big|_{f=0} \right)^2 \right]}{E \left[\left(\Delta\hat{f} \Big|_{f=0} \right)^2 \right]}. \quad (8)$$

Figure 9 shows that the proposed FD has almost the same output SNR performance as the conventional phase differential frequency detector [27]. On the other hand, the phase differential FD requires additional complicated functional blocks, such as a complex multiplier and an argument operator, while the proposed FD shares the FFT operator with the 2-D search block, resulting in a much lower hardware complexity. Therefore, the complicated operators required by the phase differential FD can be replaced with a single subtractor using the proposed algorithm.

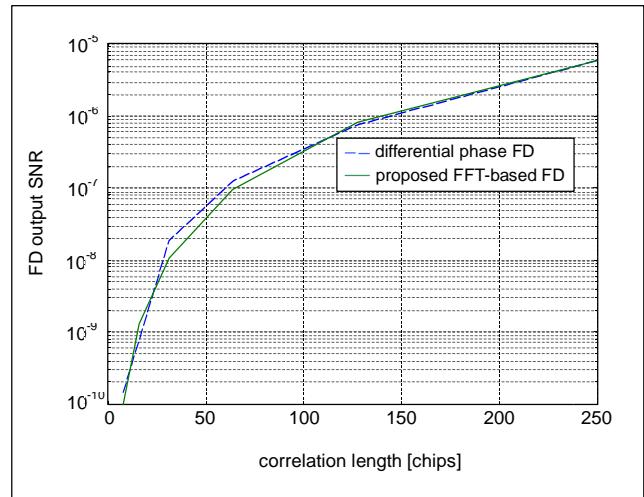


Fig. 9. FD output SNR performances of the phase differential FD and the developed FFT-based FD for a chip frequency of 4 MHz and $E_c/N_0 = -11$ dB (solid line: developed FD, dashed line: phase differential FD).

C. Simulation Results

We used simulations to evaluate the performance of the proposed Doppler shift compensation algorithm. The system parameters and variables used in the simulation are given in Table 5.

The simulation result in Fig. 10 shows the frequency error of the proposed Doppler shift compensation for the given parameters and variables. The coarse acquisition using the 2-D search successfully detected and compensated for the initial large

Table 5. System parameters for Doppler shift compensation.

| | | |
|-------------------------------|----------------------------------|--------------------------------|
| SNR (E_b/N_0) | | 19.5 dB |
| Bit rate | | 128 Kbps |
| Chip rate | | 4.096 MHz |
| Carrier frequency [GHz/band] | | 12.5 /Ku |
| Satellite orbit constellation | Satellite altitude [km] | 960 |
| | Orbit inclination [degree] | 86.4 |
| | Minimum elevation angle [degree] | 10.0 |
| Coarse acquisition | Correlation length [chips] | 4 |
| | FFT window size [chips] | 256 |
| | Number of threshold tests | 3 |
| Fine tracking | Correlation length [chips] | 32 |
| | FFT window size [chips] | 4 |
| | Gear shifting time | 12 ms after coarse acquisition |

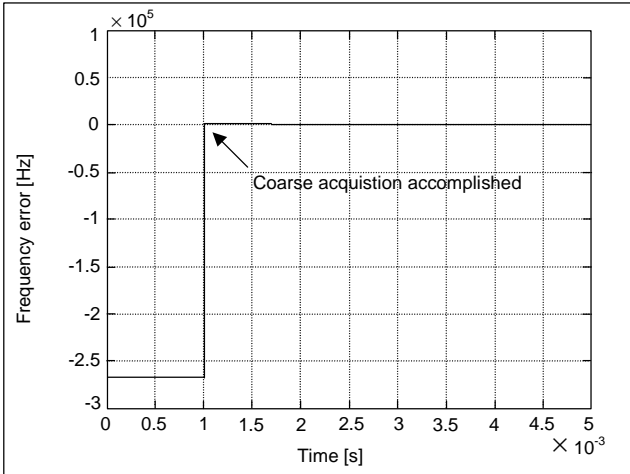


Fig. 10. The frequency error of the proposed Doppler shift compensation for the system parameters and variables given in Table 1.

Doppler shift which was about -265 kHz. After the 2-D search with the predetermined number of threshold tests, which takes about 1 ms, the frequency error was reduced to less than 8 kHz which corresponds to 1/2 of the frequency step of the FFT.

The simulation results in Fig. 11 show the frequency error of the proposed Doppler shift tracking algorithm when the residual Doppler shift after the coarse acquisition was about 1 kHz. Without gear shifting, there was an inevitable tradeoff between the convergence speed and the jitter of the residual frequency error. On the other hand, the gear-shifting technique clearly accomplished rapid initial tracking along with significantly reduced jitter of residual frequency error, where the loop filter bandwidth was designed to be changed 1 ms after the tracking loop is initiated.

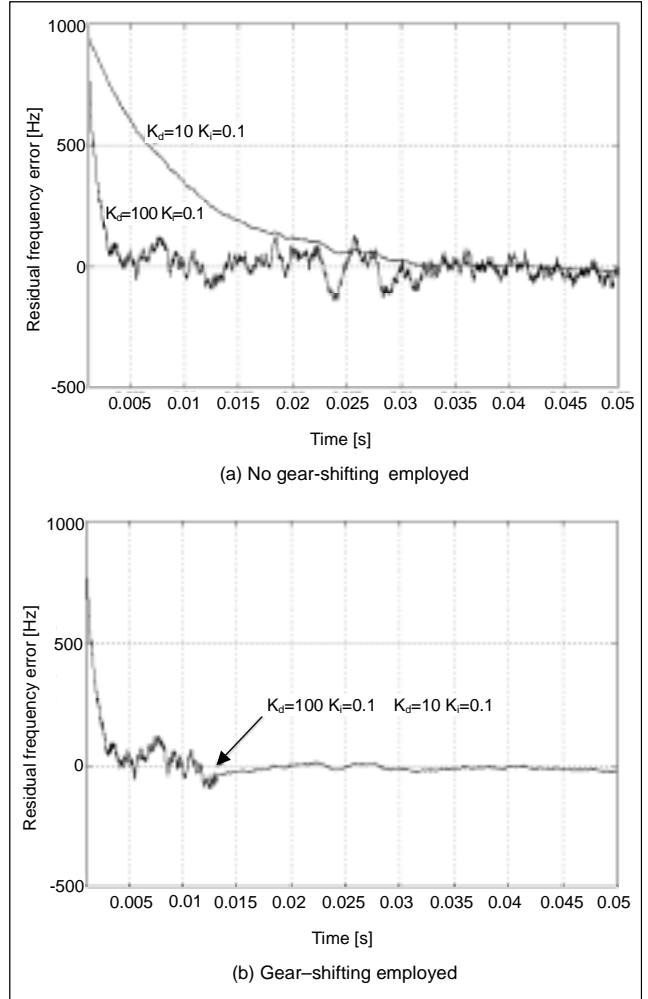


Fig. 11. Frequency error of the proposed Doppler shift tracking algorithm when the residual Doppler shift after the coarse acquisition is about 1 kHz (K_d : direct path gain of the 2nd order PLL, K_i : integration path gain of the 2nd order PLL).

IV. H/W EMULATION BOARD

We implemented our adaptive rain attenuation compensation algorithm as an H/W emulation board. The H/W emulation board for the adaptive rain fade compensation algorithm was implemented using TMS320C31 DSP chips [28]. This emulation board consisted of five modules including the link simulator 1, link simulator 2, adaptive modulator, adaptive demodulator, and BERP.

The link simulator 1 module emulates satellite communication channels; it generates rain attenuation and additive white Gaussian noise. The link simulator 2 emulates signal quality estimation, prediction and allocation of transmission schemes and output control signals to the other modules. The adaptive modulator and demodulator act as an M-ary PSK modulator and

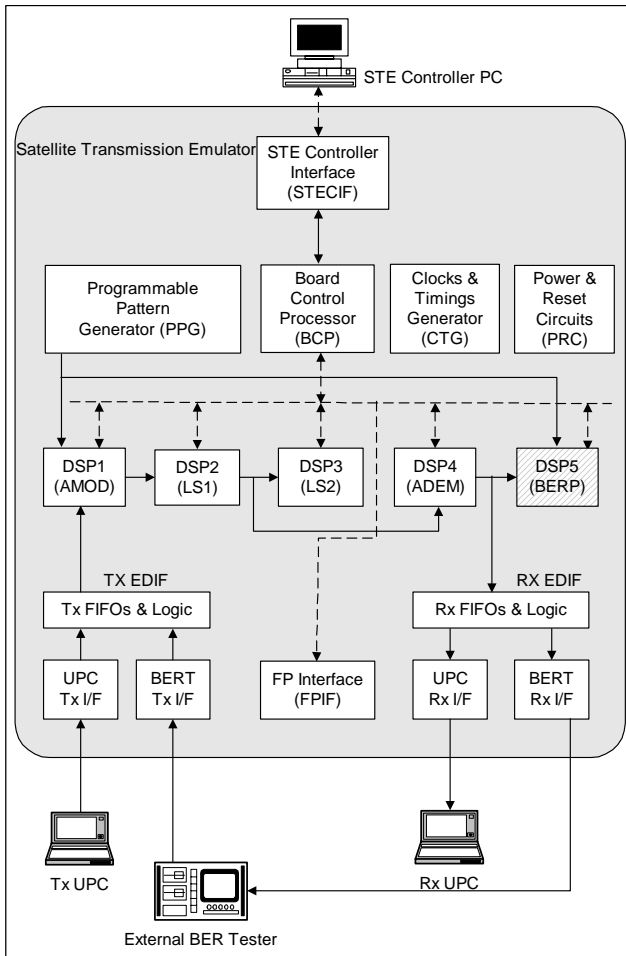


Fig. 12. The block diagram of H/W package of rain fade compensation system.



Fig. 13. The implemented H/W emulation board.

demodulator according to the control signal given by link simulator 2. The BER, throughput, and outage performance of the rain fade compensation system can be measured by the BERP module. Figure 12 shows the configuration diagram of the H/W package, and Fig. 13 shows the exterior view of the H/W emulation board. The programmable pattern generator module in Fig. 12 generates a random binary sequence.

The performance of the rain attenuation compensation algorithm can be emulated using the GUI window (graphic user interface) in the controller PC (Fig. 14). Figure 14 presents the emulation result. The emulation results from the H/W using the same system parameters as for the S/W simulation showed good agreement, having less than 1% error.



Fig. 14. The emulation result presented in graphic window at the control PC.

V. CONCLUSIONS

We have proposed an efficient adaptive rain attenuation compensation scheme and a Doppler shift compensation technique as a core technology for modern satellite communication systems.

The proposed rain attenuation compensation scheme employs an adaptive coding scheme using block turbo codes, M-ary PSK modulation schemes, and novel control algorithms. In particular, by using the SNR estimation method rather than the signal level, we achieved a good performance in signal quality estimation and prediction. The proposed radio format selection algorithm showed about 100% improvement in the change rate compared to conventional multi-threshold algorithms; and it also showed better performance in the BER and outage rate.

Overall system performance of the adaptive scheme was compared to that of the fixed schemes which have been conventionally used in satellite communication systems. The simulation results of our investigation showed that the adaptive scheme produced at least an order of magnitude improvement

in BER performance. The data throughput performance showed that the adaptive algorithm could carry about 270%, 130%, and 90% of data compared to the BPSK, QPSK, and 8-ary PSK systems, respectively. The outage rate could be reduced at least 50% by using the adaptive scheme.

The proposed Doppler shift compensation method employed a 2D-search algorithm with a gear shifting process to speed-up the initial frequency tracking. Simulation results showed that the frequency error of the proposed algorithm is in the desired range for successful demodulation with reduced hardware complexity. The proposed compensation algorithms will play an important role in providing satellite communication services which are both economical and of high quality.

REFERENCES

- [1] SkyBridge, <http://www.skybridgesatellite.com/>.
- [2] Teledesic, <http://www.teledesic.com/tech/tech.htm>.
- [3] Youngnam Han, Hang Gu Bahk, Seungtaik Yang, "CDMA Mobile System Overview: Introduction, Background, and System Concepts," *ETRI J.*, vol. 19, no. 3, Oct. 1997, pp. 83-97.
- [4] Sooyoung Kim Shin, Soo In Lee, Yang Su Kim, and Jae Moun Kim, "A Dynamic Rain Attenuation Modeling Technique for Satellite Communication Link," *Proc. of Int'l Conf. on Telecommunications*, vol. 2, June 15-18, 1999, pp. 33-37.
- [5] T. Maseng and P.M. Bakken, "A Stochastic Dynamic Model of Rain Attenuation," *IEEE Transactions on Comm.*, vol. COM-29, no. 5, pp.660-669.
- [6] R.M. Manning, "Ka-band Rain Attenuation Prediction—A New Challenge in Modeling Communication Link Performance," *Proc. of the 1st Ka-band Utilization Conf.*, Sorrento, Italy, 1995, pp. 125-146.
- [7] B.C. Gremont, A.P. Gallois, and S.D. Bate, "Efficient Fade Compensation for Ka band VSAT System," *Proc. of 2nd Ka-band Utilization Conf.*, Florence, Italy, Sep. 1996, pp. 439-443.
- [8] E.O. Elliot, "Estimates of Error Rates for Codes on Burst Noise Channels," *Bell System Tech. J.*, Sep. 1963, pp.1977-1997.
- [9] W. Lau, A. Erramilli, J.L. Wang, and W. Willinger, "Self-Similar Traffic Generation: The Random Midpoint Displacement Algorithm and its Properties," *Proc. of ICC'95*, Seattle, USA, 1995, pp. 466-472.
- [10] Sooyoung Kim Shin, Soo In Lee, and Yang Su Kim, "Interpolation Technique for Dynamic Rain Attenuation Data," *J. of Korea Institute of Comm. Sciences*, vol. 25, no. 3A, pp.317-324.
- [11] Michael J. Miller, Branka Vucetic Les Berry, *Satellite Communications: Mobile and Fixed Services*, Kluwer Academic Publishers, Boston/Dordrecht/London, 1993.
- [12] J.E. Hatleid and L. Casey, "The IRIDIUM System Personal Communications Anytime, Anyplace," *Proc. of IMSC'93*, Pasadena, CA, June 1993, pp.285-290.
- [13] A. Malygin, M. Filip, and E. Vilar, "Development of a Digital Modem for Adaptive Countermeasure VSAT System at Ka-band," *Proc. of the 2nd Ka-band utilization conf.*, Florence, Italy, Sep. 1996, pp. 277-283.
- [14] S.K. Johnson and R. Acosta, "T1 VSAT Fade Compensation Statistical Results," *Proc. of the 6th Ka-band Utilization Conf.*, Cleveland, USA, June 2000, pp. 23-29.
- [15] D. Mertens and L. Castanet, "Performance Simulation of an Adaptive Control Scheme for Scintillation Fade Compensation in a Generic Ka-band VSAT Videoconferencing System," *Proc. of the 6th Ka-band Utilization Conf.*, Cleveland, USA, June 2000, pp. 189-196.
- [16] Sooyoung Kim Shin, Ji hye Gwak, and Soo In Lee, "Adaptive Coding Scheme Using Block Turbo Codes in Satellite Communication Systems," *Proc. of JCCI2000*, vol.1, pp. 419-422.
- [17] Dong Hee Kim, Sooyoung Kim Shin, Seoung Hoon Hwang, Soo In Lee, and Kuem Chan Whang, "Adaptive CDMA Scheme for Rain Fade Compensation in Ka-band Geosynchronous Satellite Communications," *Proc. of the 5th Ka band Utilization Conf.*, 18-20 Oct. 1999, Italy, pp. 137-142.
- [18] Sooyoung Kim Shin, Kwangjae Lim, Hyoungsoo Lim, Taegon Kweon, and Soo In Lee, "Adaptive Rain Fade Compensation Technique and Its Performance Evaluation," *Proc. of the 5th CDMA Int'l Conf.*, vol. 2, Nov. 2000, pp.592-596.
- [19] Kwang-Jae LIM, Soo In LEE, and Seong Pal LEE, "Radio-Format Selection Algorithm for Rain-Fade Compensation in Adaptive Satellite Communications," *Proc. of the 6th Ka-band Utilization Conf.*, June 2000, pp.209-216.
- [20] N. Celandroni, E. Ferro, F. Potorti, "Quality Estimation of PSK Modulated Signals," *IEEE Comm. Magazine*, vol. 35, no. 7, Jul. 1997, pp. 50-55.
- [21] Paulo S.R. Diniz, *Adaptive Filtering—Algorithms and Practical Implementation*, Kluwer Academic Publishers, 1997.
- [22] M. Filip and E. Vilar, "Adaptive Modulation as a Fade Countermeasure. An Olympus Experiment," *Int'l J. of Satellite Comm.*, vol. 8, June 1990, pp. 33-41.
- [23] P.M. Grant, S.M. Spangenberg, I. Scott, S. McLaughlin, G.J.R. Prvey, and D.G.M. Cruickshank, "Doppler Estimation for Fast Acquisition in Spread Spectrum Communication Systems," *Proc. IEEE ISSSTA*, vol. 1, 1998, pp. 106-109.
- [24] U. Cheng, W.J. Hurd, and J.I. Statman, "Spread-Spectrum Code Acquisition in the Presence of Doppler Shift and Data Modulation," *IEEE Trans. Comm.*, vol. 38, no. 2, Feb. 1990, pp. 241-250.
- [25] M. Ishizu, M. Katayama, T. Yamazato, and A. Ogawa, "Initial Acquisition of Code Timings and Carrier Frequencies of CDM Down-Link Signals in Multiple-LEO-Satellite Communication Systems," *IEICE Trans. Fundamentals*, vol. E81-A, no. 11, Nov. 1998, pp. 2281-2290.
- [26] H. Lim, S.I. Lee, and S.P. Lee, "A Simple Carrier Frequency Detection Algorithm for Fine Compensation of Doppler Shift in Direct-Sequence Code Division Multiple Access Mobile Satellite Communications," *Proc. of ICC2000*, vol. 1, June 2000, pp. 109-112.
- [27] J.W. Jeong, S. Sampei, and N. Morinaga, "Large Doppler Frequency Compensation Technique for Terrestrial and LEO Satellite Dual Mode DS/CDMA Terminals," *IEICE Trans. Comm.*, vol. E79-B, no. 11, Nov. 1996, pp. 1696-1703.
- [28] Texas Instrument, "TMS320C3x-User's Guide," 1994.



Sooyoung Kim Shin received her BS degree in electrical and electronics engineering from Korea Advanced Institute of Science and Technology, Korea, in 1990. After having worked in the Satellite Communication Technology Division of ETRI, Korea, from February 1990 to September 1991, she received her MS and PhD degrees in electrical and electronics engineering

from the University of Surrey, UK, in 1992 and 1995. From November 1994 to June 1996 she was employed as a research fellow at the Centre for Satellite Engineering Research, University of Surrey, UK. In 1996 she re-joined the Satellite Communication Technology Division of ETRI, Korea. She is currently the Team Leader of the "Satellite Transmission Technology Team" and responsible for developing efficient adaptive multi-carrier transmission schemes to compensate for channel impairments in satellite communication systems. Her work also includes developing a highly efficient coding technique for digital communication systems.



Kwangjae Lim received his BS, MS and PhD degrees in electronics engineering from Inha University, Korea, in 1992, 1994 and 1999. In March 1999, he joined Electronics and Telecommunications Research Institute as a Senior Member of Research Staff. His research interests are medium access control and radio resource control in mobile satellite communications.

He is currently involved in developing adaptive resource allocation algorithms in wideband CDMA systems for IP packet services.



Kwonhue Choi received his BS, MS, and PhD degrees in electronic and electrical engineering from the Pohang University of Science and Technology (POSTECH), Korea, in 1994, 1996 and 2000. Since 2000, he has been with ETRI, Korea, and has worked for the development of efficient transmission algorithms for satellite communications. His research interests are performance analysis of CDMA networks and demodulation algorithms for digital modems.

Currently, he is involved in developing adaptive transmission algorithms for wideband CDMA systems in a fading environment.



Kunseok Kang received the BS and MS degrees in the School of Electronics and Electrical Engineering from Kyungpook National University, Korea, in 1997 and 1999. He is currently a member of research staff at Satellite Communications Application Department of ETRI, Korea, and has worked for the development of efficient transmission algorithms for satellite communications.

His research interests include satellite communications, coding technique, and multicarrier transmission.